

# Design and Control of an Autonomous Photovoltaic System with Battery Charge Regulateur using the MPPT Control Followed by PI Correctors

Essaid Ait El Maati<sup>1</sup>, Abdallah Boulal<sup>1</sup>, Ahmed Mouhsen<sup>2</sup>, Azeddine Mouhsen<sup>1</sup>

<sup>1</sup>Laboratory of radiation - matter & Instrumentation, University Hassan the first,  
Faculty of Science and Technology, Settat, Morocco

<sup>2</sup>Laboratory of Engineering, Industrial Management and Innovation, University Hassan the first,  
Faculty of Science and Technology, Settat, Morocco

**Keywords:** Autonomous photovoltaic system, battery charger, SEPIC converter, BOOST converter, PI controller, MPPT intelligent control.

**Abstract:** An Autonomous photovoltaic (PV) system requires a battery charger to store energy for consumption during the night and during days with low irradiation. This paper presents the design of the PV charger system modulator and controller implemented with the asymmetric primary inductance converter (SEPIC). The designed SEPIC is controlled by the MPPT (Pando) command to extract the maximum power of the PV generator. To the used MPPT control, a PI control regulator has been added to manage the charge loop of the battery. Subsequently, a BOOST converter has been associated with the system to adapt the output voltage of the battery to the load. The modeling of the state space is done to determine the transfer function of the converters (SEPIC and BOOST). The values of the PI correctors (Kp and Ki) are obtained using the method of Ziegler Nichols. Finally, we simulated and analyzed the performance of a 250W stand-alone photovoltaic power system on MATLAB- Simulink.

## 1 INTRODUCTION

With the depletion of fossil fuel reserves, economic crises due to soaring oil prices, accidents at nuclear power plants such as Three Mile Island (USA, 1979) and Chernobyl (USSR, 1986), as well as Fukushima (Japan 2011) public interest in renewable energies continues to grow. Of the various sources of renewable energy, photovoltaic occupies a prominent place (S. Gueye, 2014). In stand-alone photovoltaic systems, batteries are widely used to power loads in the absence of sunshine or in the event of a failure of the solar energy system. These batteries are sensitive to overload, deep discharge and temperature and current drift. It is then necessary to associate them with a regulator to ensure their protection. The importance of a charge controller in an autonomous photovoltaic system is obvious. However, it must be well designed to meet

the requirements of cost, simplicity, and reliability (S. Gueye, 2014) (S. J. Chiang, 2009).

The objective of this work is the study of an autonomous photovoltaic system with a battery charger for energy storage, controlled by an MPPT command with two PI correctors, one intended for the control of the state of charge battery discharge and the other to adapt the output voltage of the battery to the load. The article is structured as follows: we start with the presentation of the operation of the autonomous photovoltaic system, then the modeling of the state space of the converters (SEPIC and BOOST), after the method of Ziegler and Nichols is presented to determine the values of PI correctors, later we present the system control algorithm and finally the results and the discussion.

## 2 AUTONOMOUS PHOTOVOLTAIC SYSTEM

An autonomous photovoltaic system is one that produces electricity through the sun, but operates independently of the electricity grid. In the majority of cases, this system is used in isolated sites where it would be much too expensive to connect the house or the room that you want to supply with electricity. The major difference with a standard photovoltaic installation (connected to the grid) is the presence of batteries. An autonomous photovoltaic system must be able to provide energy, even when there is no more sun (at night or in bad weather). It is therefore necessary that a part of the daily production of the photovoltaic modules is stored. Below is the synoptic diagram of our autonomous photovoltaic system that consists of a GPV with a SEPIC type converter to charge the battery and a BOOST converter to power our load (S. J. Chiang,2009)(D. S. Karanjkar, S. Chatterji, S. L. Shimi, and A. Kumar, 2014).

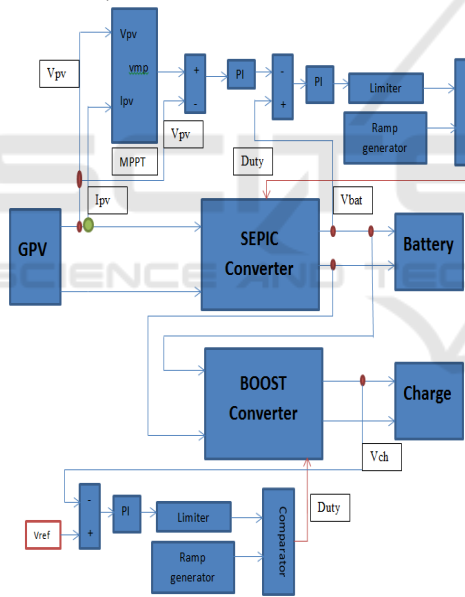


Figure 1: Synoptic diagram of the photovoltaic system

The PV module directly converts sunlight into direct current. Here, the chosen PV module is of American Solar Wholesale type ASW-250P of following

American solar wholesale ASW-250P	Value
Maximum power(W)	249.92
Open circuit volatgeVoc(V)	43,22
Short-circuitcurantIsc (A)	7.76
Voltage at maximum power point Vmp(V)	35.2
Current at maximum power point Imp(A)	7.1
Shunt resistance Rsh(ohms)	111.87
Series resistance Rsh(ohms)	0.42

characteristics:

Table 1: Characteristic of the PV module.

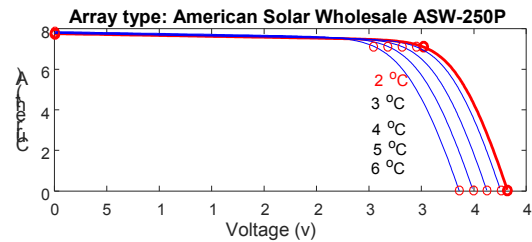


Figure 2:  $I_{pv}=f(V_{pv})$  for influence of temperature

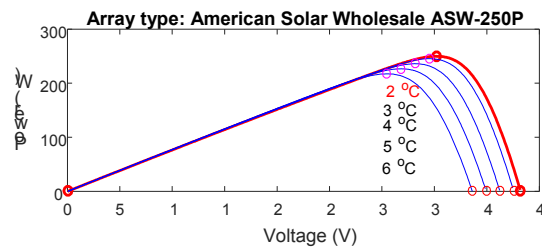


Figure 3:  $P_{pv}=f(V_{pv})$  for influence of temperature

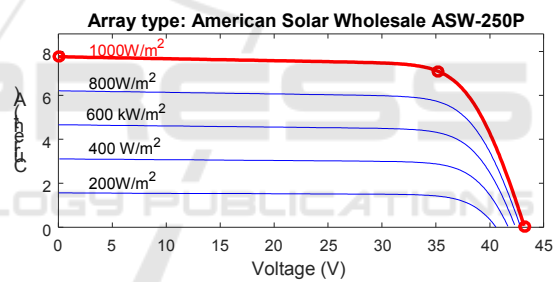


Figure 4:  $I_{pv}=f(V_{pv})$  for influence of Illumination

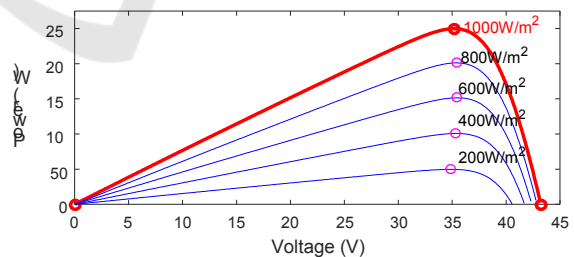


Figure 5:  $P_{pv}=f(V_{pv})$  for influence of Illumination

## 3 MODELING THE CONVERTER

### 3.1 SEPIC Converter

A SEPIC is a type of DC-DC converter allowing the electrical potential (voltage) at its output to be lower, greater or equal to that at its input.

The use of the SEPIC converter (which can play the role of a boost converter if  $\alpha > 0.5$  or step down if  $\alpha < 0.5$ ) is explained by the fact that the voltage delivered by the panel is greater than the voltage of the battery which is 24 V and has the advantage of having a non-inverted output (S. J. Chiang, 2009).

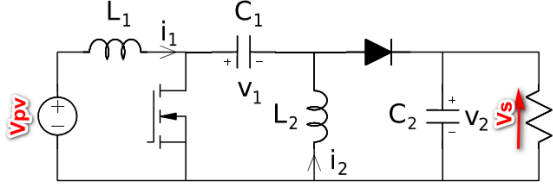


Figure 6: Circuit diagram of the SEPIC converter

For a SEPIC converter operating in continuous conduction mode (CCM), the duty cycle is given by (B. Paranthagan, 2015):

$$\alpha = \frac{V_s + V_d}{V_s + V_{pv} + V_d} \text{ with } 0 < \alpha < 1 \quad (1)$$

The PI regulator is used to monitor the state of charge-discharge of the battery and to size these parameters Ziegler and Nichols have proposed a method that requires the recording of the index response in open loop, just record the answer index of the process alone (i.e. without the regulator), then draw the tangent to the point of inflection of the curve. To do this the determination of the transfer function of the converter is mandatory.

The state space model (Chun T. Rim, Gyu B. Joung, and Gyu H. Cho, 1991) is used to determine this function. The ON state mode and the OFF state mode are given in equations (2) and (3), respectively, which can be obtained from the differential equation model (B. Paranthagan, 2015).

So if the transistor is in ON state:

$$\begin{bmatrix} \frac{dL_{L1}}{dt} \\ \frac{dL_{L2}}{dt} \\ \frac{dV_{Cs}}{dt} \\ \frac{dV_{C(OUT)}}{dt} \end{bmatrix} = \begin{bmatrix} 0 & 0 & 0 & 0 \\ 0 & 0 & \frac{1}{L_2} & 0 \\ 0 & -\frac{1}{C_1} & 0 & 0 \\ 0 & 0 & 0 & -\frac{1}{RC_{OUT}} \end{bmatrix} \begin{bmatrix} I_{L1} \\ I_{L2} \\ V_{Cs} \\ V_{C(OUT)} \end{bmatrix} + \begin{bmatrix} \frac{1}{L_1} \\ 0 \\ 0 \\ 0 \end{bmatrix} [V_{IN}] \quad (2)$$

And if the transistor is in OFF state:

$$\begin{bmatrix} \frac{dL_{L1}}{dt} \\ \frac{dL_{L2}}{dt} \\ \frac{dV_{Cs}}{dt} \\ \frac{dV_{C(OUT)}}{dt} \end{bmatrix} = \begin{bmatrix} 0 & 0 & -\frac{1}{L_1} & -\frac{1}{L_1} \\ 0 & 0 & 0 & -\frac{1}{L_2} \\ \frac{1}{C_{Cs}} & 0 & 0 & 0 \\ \frac{1}{C_{OUT}} & \frac{1}{C_{OUT}} & 0 & -\frac{1}{RC_{OUT}} \end{bmatrix} \begin{bmatrix} I_{L1} \\ I_{L2} \\ V_{Cs} \\ V_{C(OUT)} \end{bmatrix} + \begin{bmatrix} \frac{1}{L_1} \\ 0 \\ 0 \\ 0 \end{bmatrix} [V_{IN}] \quad (3)$$

In the case of a linear system, the state representation is in the form:

$$\begin{cases} \dot{x} = Ax + Bu \\ y = Cx \end{cases} \quad (4)$$

The variables:

x (t): State Vector

u (t): Vector of the entries

y (t): Vector of the outputs

A: state matrix

B: input matrix

C: output matrix

The transfer function can be written in this way by applying the Laplace transform (Marie Chantal, NiyomanziSebutimbiri, 2016):

$$\frac{Y(s)}{U(s)} = C(SI - A)^{-1}B \quad (5)$$

$$\frac{V_{OUT}}{V_{IN}} = \frac{A_1 S^3 + A_2 S^2 + A_3 S + A_4}{A_5 S^4 + A_6 S^3 + A_7 S^2 + A_8 S + A_9} \quad (6)$$

Avec:

$$A_1 = L_1 C_S L_2 \alpha \quad (7)$$

$$A_2 = L_1 C_S R \alpha^2$$

$$A_3 = -\alpha^2 L_1$$

$$A_4 = \alpha^2 R$$

$$A_5 = (1 - \alpha)^2 L_1 C_S L_2 C_{OUT} R$$

$$A_6 = (1 - \alpha)^2 L_1 C_S L_2$$

$$A_7 = (1 - \alpha)^2 R (L_1 C_S (1 - \alpha)^2 + L_1 C_{OUT} (1 - \alpha)^2 + C_S L_2 (1 - \alpha)^2 + L_1 C_{OUT} \alpha^2)$$

$$A_8 = (1 - \alpha)^2 (L_2 (1 - \alpha)^2 + L_1 \alpha^2)$$

$$A_9 = (1 - \alpha)^4 R$$

For our study we apply the values of Table 2 obtained after sizing of our converter or I determine the constants of the model (6).

The values of the inductances are calculated as follows:

$$L_1 = L_2 = \frac{V_{pv}}{\Delta I_L \times f_{sw}} \quad (8)$$

The values of the output and coupling capacitors are calculated as follows:

$$C_s \geq \frac{I_s}{V_{Cs \text{ ripple}} \times 0.5 \times f_{sw}} \times \alpha \quad (9)$$

$$C_c = \frac{i_s \alpha}{\Delta u_{Cc} \times f_{sw}} \quad (10)$$

Table 2: Dimensioning of the SEPIC converter.

SEPIC converter parameters	Value
Cyclic duty $\alpha$	0,41
Cutting frequency	100KHz
Value of inductance (L1 et L2)	200 $\mu$ H
Output capacitor	1000 $\mu$ F
Coupling capacitor	47 $\mu$ F
Input voltage $V_{pv}$	35.2V
Output voltage $V_{out}$	24V
Power $P_{pv}$	250W

The following figure illustrates the open-loop step response of the SEPIC converter.

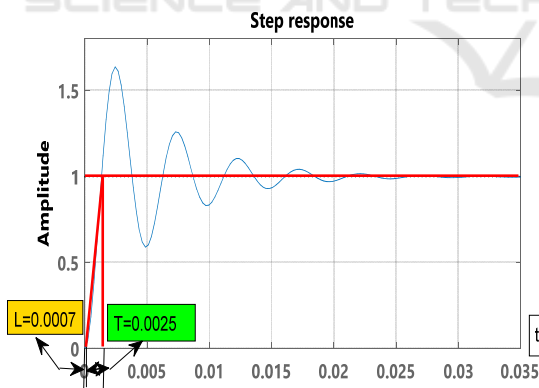


Figure 7: Open loop index response of the SEPIC converter

From the index response, the two constants namely the delay time  $L = 0.0007s$  and the time constant  $T = 0.0025s$  are obtained.

The transfer function of the PI controller is written in general form:

$$\frac{U(s)}{E(s)} = k_p + \frac{k_i}{s} = k_p \left(1 + \frac{1}{T_{is}}\right) \quad (11)$$

Using the Ziegler and Nichols settings, we obtain the values of our PI controller (Smitha K, 2012) (Mitulkumar R, 2012):

$$K_p = \frac{0.9T}{L} = 3.21 \quad (12)$$

$$T_i = \frac{L}{0.3} = 0.0023 \text{ s} \quad (13)$$

### 3.2 Modelling of the BOOST Converter

With this type, the average output voltage  $V_2$  is greater than that of the input  $V_1$ . The use of the BOOST converter is for the sake of adapting the output voltage of the battery to the load (S.S.Shinde, 2016).

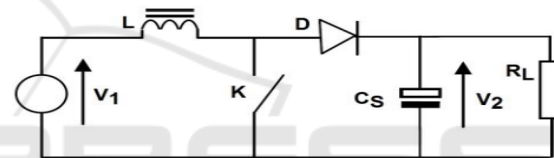


Figure 8: Circuit diagram of the Boost converter

The duty cycle in CCM mode is given by:

$$\alpha = \frac{V_1 - V_2}{V_2} \text{ avec } 0 < \alpha < 1 \quad (14)$$

To adapt the output voltage of the battery to the load the PI regulator is used, these parameters are obtained by the use of Ziegler and Nichols method.

To make this study the determination of the transfer function of the converter is mandatory. Following the same procedure of the SEPIC converter we have (Smitha K, 2012):

If the transistor is in the ON state:

$$\begin{bmatrix} \dot{x}_1 \\ \dot{x}_2 \end{bmatrix} = \begin{bmatrix} 0 & 0 \\ 0 & -\frac{1}{RC} \end{bmatrix} \begin{bmatrix} x_1 \\ x_2 \end{bmatrix} + \begin{bmatrix} \frac{1}{L} \\ 0 \end{bmatrix} V_{pv} \quad (15)$$

If the transistor is in the OFF state:

$$\begin{bmatrix} \dot{x}_1 \\ \dot{x}_2 \end{bmatrix} = \begin{bmatrix} 0 & -\frac{1}{L} \\ \frac{1}{C} & -\frac{1}{RC} \end{bmatrix} \begin{bmatrix} x_1 \\ x_2 \end{bmatrix} + \begin{bmatrix} \frac{1}{L} \\ 0 \end{bmatrix} V_{pv} \quad (16)$$

By application of the Laplace transform (Marie Chantal, Niyomanzi Sebutimbiri, 2016), the transfer function is written as:

$$\frac{V_s}{V_{pv}} = \frac{\alpha}{RC(1-\alpha)^2} \times \frac{\frac{R(1-\alpha)^2}{L} - S}{S^2 + \frac{S}{RC} + \frac{(1-\alpha)^2}{LC}} \quad (17)$$

The values of Table 3 are obtained after sizing of our converter where I determine the constants of the model (17).

The value of the inductance is calculated as follows:

$$L = \frac{\alpha \times V_{bat}}{f_{sw} \times \Delta I} \quad (18)$$

The value of the output capacitor is calculated as follows:

$$C_s = \frac{I_s \alpha}{f_{sw} \Delta V_{Cs}} \quad (19)$$

Table 3: Dimensioning of the BOOST converter.

BOOST converter parameters	Value
Cyclic duty $\alpha$	0,5
Cutting frequency	100KHz
Value of inductance L1	200 $\mu$ H
Output capacitor	47 $\mu$ F
Input voltage Vbat	24V
Output voltage Vs	48V
Charge R	10 $\Omega$

From the step response, the two constants namely the delay time  $L = 0.0005s$  and the time constant  $T = 0.005s$  are obtained.

The following figure illustrates the open-loop step response of the BOOST converter.

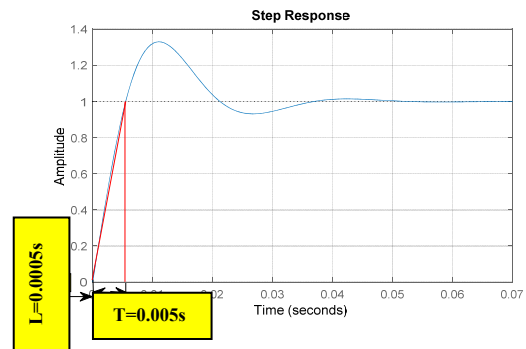


Figure 9: Open loop step response of the BOOST converter

The transfer function of the PI controller is written in general form:

$$\frac{U(s)}{E(s)} = k_p + \frac{k_i}{s} = k_p \left(1 + \frac{1}{T_i s}\right) \quad (20)$$

Using the Ziegler and Nichols settings, we obtain the values of our PI controller (Smitha K, 2012) (Mitulkumar R, 2012):

$$K_p = \frac{0.9T}{L} = 9 \quad (21)$$

$$T_i = \frac{L}{0.3} = 0.0016 \text{ s} \quad (22)$$

## 4 DIMENSIONING BATTERY VOLTAGE

We recall that a battery consists of several electrochemical conversion elements. Each element is considered as a voltage generator of 2V. By stacking these elements, one obtains batteries of 6V, 12V, 24V or 48V.

In order to determine the appropriate voltage of the battery, it is appropriate to be placed in the most unfavorable configuration, that is to say when the batteries completely power the electrical equipment (without any contribution of the photovoltaic field) (S.S.Shinde,2016) (C. de Manuel, J. Cubas, and S. Pindado,2014).

The mathematical formula for determining the battery voltage is shown below:

$$(23)$$

$$V_{bat} = \sqrt{\frac{\rho \times 2 \times L \times P}{S \times \epsilon}}$$

Avec:

- **ρ**: resistivity of the conductive material (copper or aluminum) under operating temperature conditions, expressed in Ω.mm<sup>2</sup> / m. We can consider that  $\rho = 1.25 \times \rho_0$  where  $\rho_0$  is the resistivity of the conductor at 20 ° C.
- **L**: Length of the cables connecting the battery to the distribution board, expressed in m. The factor 2 makes it possible to take into account the distances to and from the cable.
- **P**: is the electrical power, expressed in W.
- **S**: Cable cross-section between the battery and the distribution board, in mm<sup>2</sup>.
- **ε**: Voltage drop tolerated between the battery and the distribution board.

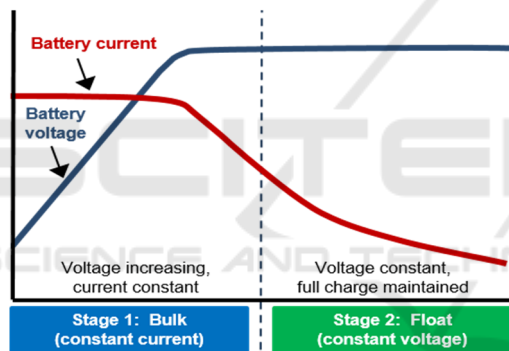


Figure 10: Battery charge profile

In our case we used a voltage battery:

$$V_{bat} = 24V \tag{24}$$

### 4.1 Calculation of the Nominal Capacity of the Battery

The nominal capacity of the battery, noted CN (C10), makes it possible to quantify the autonomy of the battery vis-à-vis the electrical consumption of the equipment.

$$C_{10} = \frac{\text{Autonomie} \times \text{Energie journalier}}{1 - \alpha_f} \tag{25}$$

With:

- $\alpha_f$ : Desired end state of charge

### 4.2 Determination of Charging Time

The charging time T is the time required for recharging a battery can be estimated by calculation

$$T = \frac{Q}{I} \tag{26}$$

- Q: the maximum electric charge of a battery announced in amperes-hours (Ah)
- I: The rated load current I

For our case we use a battery with an energy capacity of 7 Ah with a nominal load of 1A so:

$$T = \frac{7}{1} = 7h \tag{27}$$

## 5 MAXIMUM POWER POINT TRACKING (MPPT)

The MPPT command, "Maximum Power Point Tracking", is an essential control for optimal operation of the photovoltaic system. The principle of this control is based on the automatic variation of the duty cycle by bringing it to the optimum value in order to maximize the power delivered by the PV panel. For this reason, we will present and study the PandO algorithm (M.R. Sourov, U.T. Ahmed and M.G. Rabbani, 2012) ( M. Azab, 2009).

### 5.1 Algorithm of the PandO Command

The perturb and observe control (PandO) is used to extract the maximum power of the PV generator whatever the variation of the irradiation and the temperature (D. S. Karanjkar, S. Chatterji, S. L. Shimi, and A. Kumar, 2014).

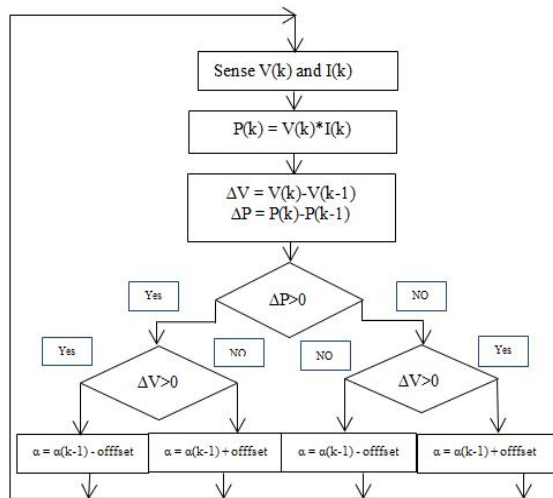


Figure 11: PandO algorithm

### 5.2 PI Controller

In this way the systems are intended to ensure equality (or at least the smallest error) between the set point and the output.

The controller P will reduce the rise time and reduce the static error, without eliminating it completely. An I controller will eliminate the static error, but can make the transient response worse. The D controller will increase the stability of a system, reduce overshoot and can improve the transient response (Mitulkumar R, 2012).

The goal of using the PI controllers is to monitor the state of charge and discharge of the battery and to adapt the output voltage of the battery to the load (Smitha K, 2012).

And the parameters of the PI controllers used are grouped in the table below:

Table 4: Table Ziegler and Nichols tuning.

Parameters of PI controller	Kp	Ti
Parameters of PI controller for SEPIC converter	3.21	0.0023
Parameters of PI controller for BOOST converter	9	0.0016

## 6 SIMULATION RESULTS

The simulation results presented in this section are developed using Matlab/SIMULINK. The battery voltage used has a nominal voltage of 24V. A resistive load of 10 Ω is used for the simulation.

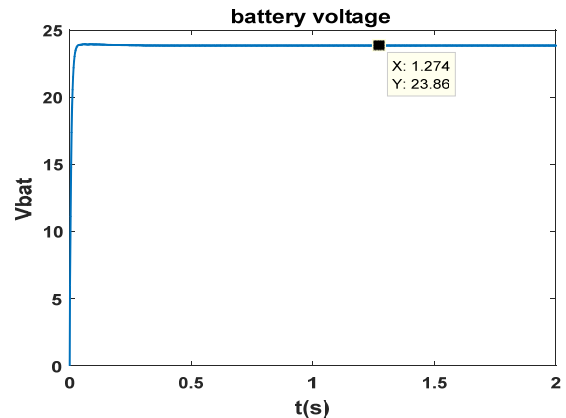


Figure 12: The battery voltage

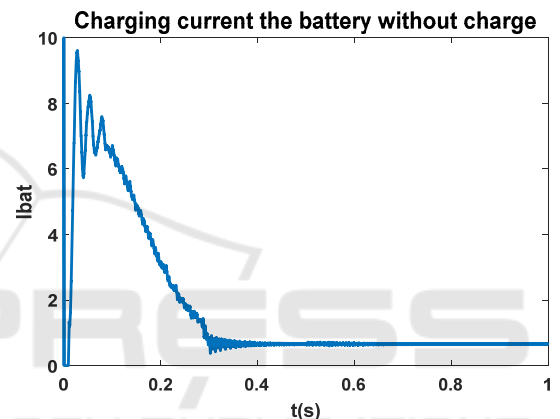


Figure 13: Charging current of the battery

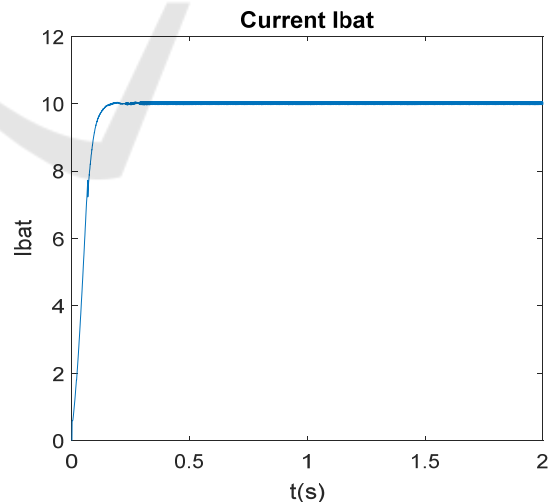


Figure 14: Ibat current of the battery with charge

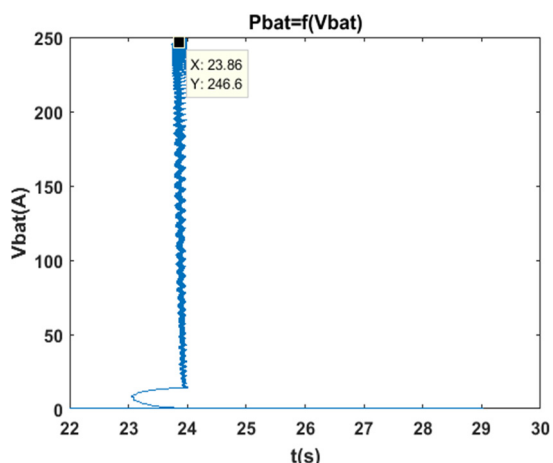


Figure 15: The power  $P_{bat}$  according to  $V_{bat}$

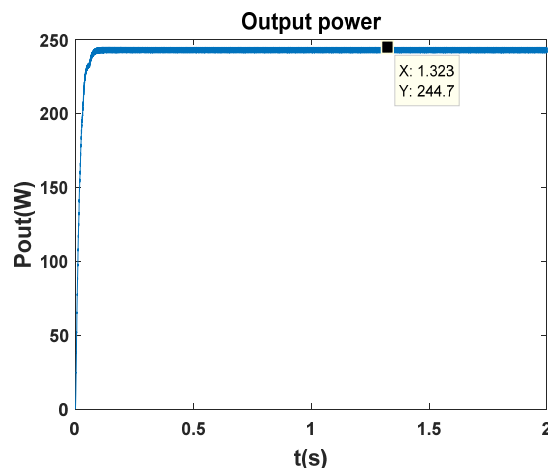


Figure 18: Output power of the PV system

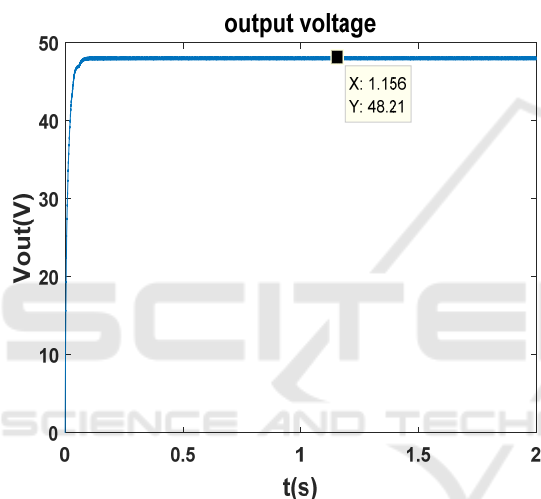


Figure 16: The output voltage of the PV system

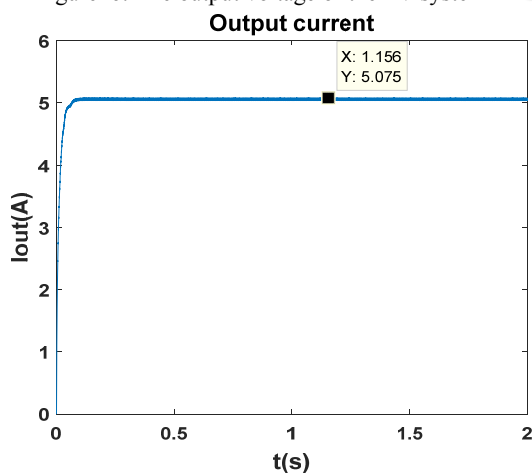


Figure 17: Output current of the PV system

## 7 DISCUSSION

The simulation results have shown that the charge-discharge regulator of the battery has good regulating capacity by the use of the SEPIC converter, the voltage  $V_{bat}$  is of the order of 23.86 V with a response time of 0.08 s and a ripple rate of 1%. The current  $I_{bat}$  with charge is stabilized at 10, 34A that is to say with a power of 246.7124 and a yield of 98.6%.

For the boost converter model “Figure 16” shows the output voltage response of the BOOST converter for an input voltage of 24 V with an output load of 10  $\Omega$ . The controller PI stabilizes the output voltage  $V_s$  compared with the reference voltage 48V. According to the simulation, after 0.1s, the output voltage is restored to its reference value with a ripple rate of 1% in the steady state. The efficiency of the converter is of the order of 98%, that is to say an output power of 244,7W for a load of 10 $\Omega$ .

The following table summarizes the main specifications of the PV and previously studied MPPT algorithms.

Table 5: PV performance based on luminal radiation.

PV	$P_{pvmax}$	$I_{cc}$	$V_{co}$	$N_s$	$N_p$
1kW/m <sup>2</sup>	250W	7.76A	43.2V	10	6

Table 6: Analysis the performance of PV system.

Parameters PV System	Value
Maximum power extracted	244.7W
Voltage at the battery terminal Vbat(V)	24V
Output voltage Vout(V)	48,21V
Response time Vbat	0.1s
Response time Vs	0.1s
% of Overshoot Vs	1%
% of Overshoot Vbat	0%
Efficiency%	98%
Observation	GOOD in response and power transmitted

## 8 CONCLUSION

In this article we have described the main elements of the autonomous PV system. Then, we dimensioned the parameters of the PI correctors by the use of the state space method to define the transfer function of the following converters: SEPIC and BOOST and after the use of the Ziegler and Nichols method to define the values of Kp and Ki. Finally, we finished with a simulation of the autonomous PV system. The results of the simulations show that the system has an efficiency of 97% with a ripple rate of 1% and a response time of 0.1s. The use of the SEPIC converter with the MPPT command followed by the PI controllers shows that the system has good regulation capacity, the voltage Vbat is of the order of 23.86 V with a response time of 0.08 s and a ripple rate of 1%. The current Ibat is stabilized at 10, 34A that is to say the power is of the order of 246.7124 and the efficiency is equal to 98.6%. The BOOST converter is used to adapt the output voltage of converter SEPIC At the voltage demand by the load, the result shows that the converter has good performance: an efficiency of the order of 97% that is to say an output power of 242W for a load of 10Ω

## REFERENCES

S. Gueye, 2014. "Conception d'un régulateur solaire avec commande MPPT" Laboratoire d'Energies Renouvelables, Ecole supérieure Polytechnique, Université Cheikh AntaDiop de Dakar - BP 5085 (Dakar, Senegal) Vol. 1(2) ISSN 2312-8712.  
 B. Paranthagan, 2015. "Comparative Analysis of Performance of the SEPIC Converter Using PID and

Fuzzy Logic Controllers for LED Lighting Applications" International Journal of Emerging Technology in Computer Science & Electronics (IJETCSE) ISSN: 0976-1353 Volume 12 Issue 2.  
 S. J. Chiang,2009. "Modeling and Control of PV Charger System With SEPIC Converter" iee transactions on industrial electronics, vol. 56, no. 11.  
 S.S.Shinde,2016. "Performance Analysis of Boost Converter Using Fuzzy Logic and PID Controller" IOSR Journal of Electrical and Electronics Engineering (IOSR-JEEE) e-ISSN: 2278-1676,p-ISSN: 2320-3331, Volume 11, Issue 3 Ver. I.  
 Smitha K, 2012. "Steady State Analysis of PID Controlled Boost Converter using State Space Averaging Technique" National Conference-NCPE-2k15, organized by KLE Society's Dr. M. S. Sheshgiri College of Engineering & Technology, Belagavi, Special issue published by Multidisciplinary Journal of Research in Engineering and Technology, Pg.100-110.  
 Mitulkumar R, 2012. "Analysis of Boost Converter Using PI Control Algorithms" International Journal of Engineering Trends and Technology- Volume 3 Issue 2.  
 M.R. Sourov, U.T. Ahmed and M.G. Rabbani,2012. 'A High Performance Maximum Power Point Tracker for Photovoltaic Power System Using DC-DC Boost Converter', IOSR Journal of Engineering, Vol. 2, N°12, pp. 12 – 20.  
 M. Azab,2009. 'A New Maximum Power Point tracking for Photovoltaic Systems', International Journal of Electrical and Electronics engineering, vol. 3, N°11.  
 D. S. Karanjkar, S. Chatterji, S. L. Shimi, and A. Kumar, 2014. "Real time simulation and analysis of maximum power point tracking (MPPT) techniques for solar photo-voltaic system," in Proceed-ings of the Recent Advances in Engineering and Computational Sciences (RAECS '14), pp. 1–6.  
 D. Zhou and C. Chen,2015. "Maximum power point tracking strategy based on modified variable step-size incremental conductance algorithm," Power System Technology, vol. 39, no. 6, pp. 1492–1498.  
 Marie Chantal, NiyomanziSebutimbiri, 2016. "Sur Quelques Applications de la Transformation de Laplace" International Journal of Innovation and ScientificResearch ISSN 2351-8014 Vol. 21 No. 2, pp. 342-350.  
 C. de Manuel, J. Cubas, and S. Pindado,2014. "On the simulation of the UPMSat-2 microsatellite power," in Proceedings of the European Space Power Conference, pp. 1–7.  
 M.R. Sourov, U.T. Ahmed and M.G. Rabbani,2012. 'A High Performance Maximum Power Point Tracker for Photovoltaic Power System Using DC-DC Boost Converter', IOSR Journal of Engineering, Vol. 2, N°12, pp. 12 – 20.  
 Kureve,2017. "A Sepic Type Switched Mode Power Supply System For Battery Charging In An Electric Tricycle (Auto Rickshaw)" international journal of scientific & technology research volume 6, issue 08.

Chun T. Rim, Gyu B. Joung, and Gyu H. Cho,1991."|  
Practical Switch Based State Space Modeling of DC

DC Converters with All Parasitics",| IEEE Trans. on  
power electronics, vol. 6 No. 4.

